Available online at www.sciencedirect.com

ScienceDirect

www.elsevier.com/locate/brainres

Research Report

Evidence for rostro-caudal functional organization in multiple brain areas related to goal-directed behavior

Matthew L. Dixon[a,*], Kieran C.R. Fox[a], Kalina Christoff[a,b]

[a]Department of Psychology, University of British Columbia, 2136 West Mall, Vancouver, BC, Canada V6T 1Z4
[b]Brain Research Centre, University of British Columbia, Vancouver, BC, Canada V6T 1Z4

ARTICLE INFO

Article history:
Accepted 10 May 2014
Available online 16 May 2014

Keywords:
Lateral prefrontal cortex
Medial prefrontal cortex
Cingulate
Insula
Rules
Action
Goals
Motivation
Rostro-caudal organization

ABSTRACT

The functional organization of brain areas supporting goal-directed behavior is debated. Some accounts suggest a rostro-caudal organization, while others suggest a broad recruitment as part of a multiple demand network. We used fMRI and an anatomical region of interest (ROI) approach to test which account better characterizes the organization of key brain areas related to goal-directed behavior: the lateral prefrontal cortex (LPFC), medial prefrontal cortex (MPFC), cingulate cortex, and insula. Subjects performed a cognitive control task with distinct trial events corresponding to rule representation, rule maintenance, action execution, and monitoring progress towards an overarching motivational goal. The use of ROIs allowed us to look for evidence of rostro-caudal gradients during each event separately. Our results provide strong evidence for rostro-caudal gradients in all regions. During the action execution period, activation was robust in caudal ROIs and decreased linearly moving to rostral ROIs in the LPFC, cingulate cortex, and MPFC. Conversely, during the goal monitoring period, activation was weak in caudal ROIs and increased linearly moving to the rostral ROIs in the aforementioned regions. The insula exhibited the reverse pattern. These findings provide evidence for rostro-caudal organization in multiple regions within the same study. More importantly, they demonstrate that rostro-caudal gradients can be observed during individual trial events, ruling out confounding factors such as task difficulty.

1. Introduction

Goal-directed behavior involves the representation of a motivational goal (i.e., a desired outcome), forming rules for guiding actions, physical execution of those actions, and monitoring feedback indicating progress towards the motivational goal. The neural network underlying these processes includes the lateral prefrontal cortex (LPFC), insula, cingulate cortex, and medial prefrontal cortex (MPFC), among other regions (Badre and D'Esposito, 2007; Bunge et al., 2003; Cole and Schneider, 2007; Dixon and Christoff, 2012, 2014; Dosenbach et al., 2006; Duncan, 2010; Koechlin et al., 2003; Kouneiher et al., 2009; Rushworth et al., 2007). A fundamental goal for cognitive neuroscience is understanding the precise functional organization of these

*Corresponding author. Fax: +1 604 822 6923.
E-mail addresses: mattdixon@psych.ubc.ca (M.L. Dixon), kfox@psych.ubc.ca (K.C.R. Fox), kchristoff@psych.ubc.ca (K. Christoff).

http://dx.doi.org/10.1016/j.brainres.2014.05.012
0006-8993/

regions. Two prominent theories have been put forth, providing two contrasting perspectives.

The rostro-caudal organization theory suggests that rostral parts of a given area support different (usually more complex) functions than caudal parts. For example, evidence suggests that the caudal LPFC supports simple concrete rules for action, whereas rostral LPFC supports more abstract rules and goals (Badre, 2008; Badre and D'Esposito, 2007, 2009; Christoff and Gabrieli, 2000; Christoff and Keramatian, 2007; Christoff et al., 2009; Eiselt and Nieder, 2013; Koechlin et al., 2003; Kouneiher et al., 2009; Petrides, 2005; Race et al., 2009). One model of dorsal cingulate/MPFC functional organization (Venkatrama et al., 2009) suggests that caudal areas regulate action execution, whereas rostral areas support high-level decision making and strategic processes (for an alternate model see Kouneiher et al., 2009). Finally, the posterior insula has been implicated in sensory-motor and interoceptive processes (e.g., viscero-somatic sensations related to heartbeat and respiration), whereas the anterior insula may integrate this viscero-somatic information with higher-order cognitive information during goal-directed action (Craig, 2002; Critchley et al., 2004; Dosenbach et al., 2006; Farb et al., 2013; Menon and Uddin, 2010; Singer et al., 2004).

An alternative theory suggests that brain areas related to goal-directed behavior are broadly recruited as part of a 'multiple demand' network to support current task demands (Crittenden and Duncan, 2014 Duncan, 2010; Farooqui et al., 2012). According to this theory, task relevant information is represented by a distributed pattern of activity in each of these brain areas, and does not conform to a rostro-caudal gradient. Evidence for this theory includes the finding that simple task difficulty manipulations can result in widespread increases in multiple demand network activation (Crittenden and Duncan, 2014). Reynolds and colleagues have also provided evidence that the LPFC is not organized along a rostro-caudal axis, but rather, is sensitive to temporal dynamics, exhibiting either transient or sustained activation depending on task demands (Reynolds et al., 2012).

The present study used functional magnetic resonance imaging (fMRI) to test which theoretical account better characterizes the functional organization of the LPFC, insula, cingulate cortex, and MPFC. We examined activation patterns during a cognitive control task composed of several distinct trial events relevant to goal-directed behavior: (1) rule representation; (2) rule maintenance; (3) action execution; and (4) monitoring progress towards an overarching motivational goal (earning $60 by the end of the experiment) (see Fig. 1 and Section 4).

Our study expands upon prior work in several important ways. First, prior studies have typically used different task conditions to look for rostro-caudal organization (e.g., low versus high complexity rule demands). However, one limitation of this approach is that the conditions often differ in difficulty, complicating the interpretation of observed differences in activation between rostral and caudal regions. To avoid this problem, we used *a priori* defined regions of interest (ROIs) (see Fig. 2 and Table 1), and compared activation levels in rostral and caudal ROIs during the *identical* trial event (e.g., during action execution). This allows for a straightforward interpretation of results: if rostral and caudal regions have different functions, then they should respond differently to the identical event. Additionally, prior studies have often examined the LPFC as a whole, whereas we partitioned the LPFC into its constituent gyri (inferior, middle, and superior) and examined each as a separate rostro-caudal stream. This may provide more insight into the specific functional organization of the LPFC, which is pertinent given a recent study showing that the ventral and dorsal LPFC exhibit separate (parallel) rostro-caudal patterns of functional connectivity with the cingulate cortex/MPFC (Blumenfeld et al., 2012). Furthermore, the ROI approach allowed us to examine rostro-caudal organization during several distinct trial events in a theoretically agnostic manner, thereby revealing the component of goal-directed behavior to which each brain area is most sensitive.

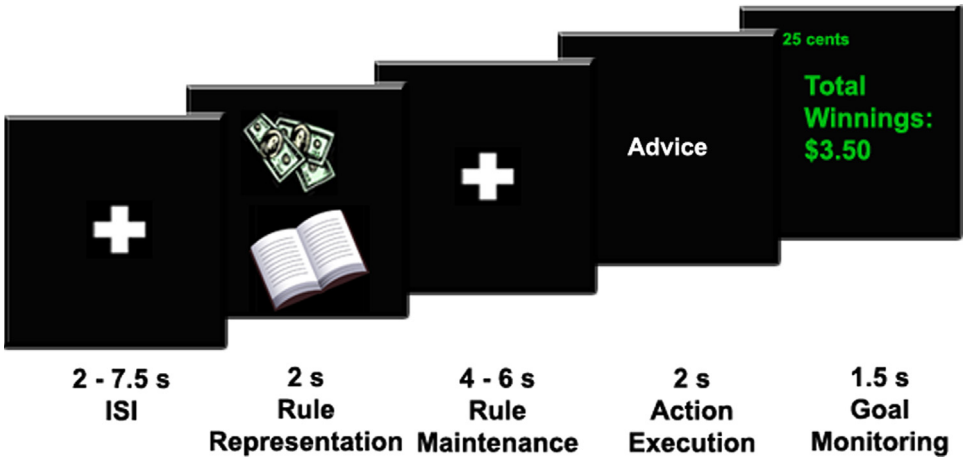

Fig. 1 – Illustration of the trial events. After a variable duration fixation cross, there was a 'rule representation' period during which an instruction cue signaled the currently relevant rules (e.g., book = abstract/concrete rule) and whether or not to expect a monetary reward (e.g., bills = 25¢). This was followed by a variable duration delay period ('rule maintenance'). Then a word or face stimulus appeared, and participants made a button response ('action execution'). Finally, a screen revealed whether money had been earned on that trial and cumulative winnings; participants were told to focus on their progress towards the overarching motivational goal of earning the maximum amount of money possible, which was $60 ('goal monitoring').

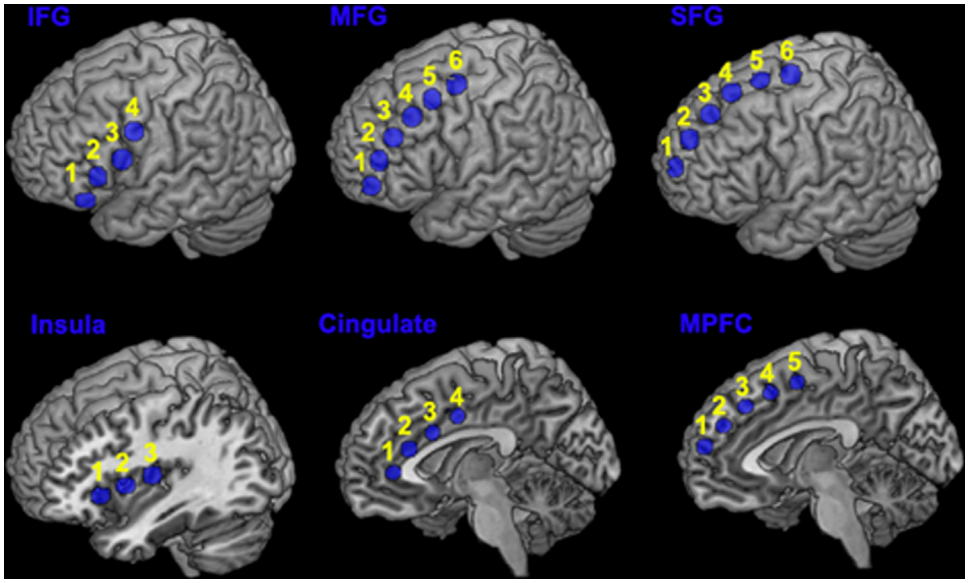

Fig. 2 – Illustration of the regions of interest (ROIs). IFG: 1. pars orbitalis (area 47/12), 2. pars triangularis (area 45), 3. pars opercularis (area 44), 4. vPMC (area 6v). MFG: 1. ventral rLPFC (area 10), 2. rLPFC (area 10/46), 3. mid-dLPFC (area 46), 4. mid-dLPFC (area 9/46), 5. caudal dLPFC (area 8A), dPMC (area 6d). SFG: rLPFC (area 10), 2. rLPFC (area 10), 3. mid-dLPFC (area 9), 4. mid-dLPFC (area 9), 5. caudal dLPFC (area 8B), dPMC (area 6d). Insula: 1. anterior insula, 2. mid-insula, 3. posterior insula. Cingulate: 1. pgACC (area 24), 2. aMCC (area a24′), 3. aMCC (area a24′), 4. pMCC (area p24′). MPFC: 1. rMPFC (area 10), 2. dMPFC (area 9), 3. dMPFC (area 8B), 4. pre-SMA (area 6), 5. SMA (area 6). See Table 1 for the complete ROI names corresponding to the abbreviations.

2. Results

Statistical results of the ROI analysis are presented in Table 2.

2.1. *Behavioral data*

On average participants earned $59.23, with five participants earning the maximum amount of money ($60). The median reaction time (RT) across all trials was 829.22 ms (SD=76.52) and the average accuracy was very high at 97.90% (SD=1.32%). There was no difference ($p>0.3$) in median RT for the male/female rule (843.25 ms; SD=78.61 ms) and for the abstract/concrete rule (827.43 ms; SD=81.20 ms). Importantly, participants were faster to respond when money was available as compared to when no money was available to be earned (*Mean RT diff*=41.12 ms, SD=56.56 ms) [$t(14)=2.82$, $p=0.014$; two-tailed]. There was no difference in accuracy ($p>0.3$). This incentive effect suggests that subjects were paying attention to every instruction cue and using them to prepare for each trial.

2.2. *Rule representation*

Fig. 3 illustrates percent signal change values for each ROI during the rule representation period. Rostro-caudal organization was observed in the inferior frontal gyrus (IFG) and the medial prefrontal cortex (MPFC). Activation increased linearly from rostral (pars orbitalis; area 47/12) to caudal (ventral premotor cortex; area 6v) in the left hemisphere of the IFG. Similarly, activation progressively increased from rostral (rostromedial prefrontal cortex; area 10 m) to caudal (supplementary motor cortex; area 6) in the MPFC. There was also a tendency for activation to increase from rostral (pregenual anterior cingulate, area 24) to caudal (posterior mid-cingulate, area p24′) in the cingulate cortex, although activation magnitude was similar in the two most caudal ROIs. The remaining areas did not exhibit clear rostro-caudal organization during rule representation.

2.3. *Rule maintenance*

Fig. 4 illustrates percent signal change values for each ROI during the rule maintenance period. Rule maintenance activation was relatively weak in all of the brain areas examined, and generally speaking, did not vary much across ROIs. However, activation did decrease linearly from rostral to caudal in the IFG and insula.

2.4. *Action execution*

Fig. 5 illustrates percent signal change values for each ROI during the action execution period. Rostro-caudal organization was observed in several areas. A strong rostro-caudal gradient was present in the IFG, with activation increasing linearly from rostral to caudal. Both pars opercularis (area 44) and the ventral premotor cortex (area 6v) exhibited robust action execution activation. Similarly, clear rostro-caudal organization was present in the cingulate cortex, with activation showing a linear increase from rostral to caudal. Notably, activation was particularly robust in the cingulate ROIs located nearest to the cingulate motor areas (Morecraft and Tanji, 2009; Picard and Strick, 1996). The MPFC also demonstrated a linear trend reflecting an increase in activation from rostral to caudal, with strong activation in the pre-supplementary and supplementary motor areas. The

Table 1 – Labels and coordinates for the regions of interest (ROIs).

ROI	Area	X	Y	Z
Ventrolateral prefrontal cortex				
Pars orbitalis	47/12	±50	35	−10
Pars triangularis	45	±55	28	7
Pars opercularis	44	±59	13	19
Ventral premotor cortex (vPMC)	6v	±56	5	36
Middle frontal gyrus				
Ventral rostrolateral prefrontal cortex (rLPFC)	10	±40	55	−2
Rostrolateral prefrontal cortex (rLPFC)	10/46	±42	50	15
Mid dorsolateral prefrontal cortex (mid-dLPFC)	46	±42	41	30
Mid dorsolateral prefrontal cortex (mid-dLPFC)	9/46	±42	29	43
Caudal dorsolateral prefrontal cortex (caudal dLPFC)	8A	±40	16	53
Dorsal premotor cortex (dPMC)	6d	±33	−1	59
Superior frontal gyrus				
Rostrolateral prefrontal cortex (rLPFC)	10	±22	66	13
Rostrolateral prefrontal cortex (rLPFC)	10	±20	56	30
Mid dorsolateral prefrontal cortex (mid-dLPFC)	9	±20	43	46
Mid dorsolateral prefrontal cortex (mid-dLPFC)	9	±18	29	59
Caudal dorsolateral prefrontal cortex (caudal dLPFC)	8B	±18	11	67
Dorsal premotor cortex (dPMC)	6d	±22	−8	70
Insula				
Anterior insula		±36	23	0
Mid insula		±39	7	6
Posterior insula		±40	−10	12
Cingulate cortex				
Pregenual anterior cingulate (pgACC)	24	0	40	5
Anterior mid-cingulate (aMCC)	a24′	0	30	20
Anterior mid-cingulate (aMCC)	a24′	0	15	30
Posterior mid-cingulate (aMCC)	p24′	0	−1	40
Medial prefrontal cortex				
Rostromedial prefrontal cortex (rMPFC)	10	0	60	18
Dorsomedial prefrontal cortex (dMPFC)	9	0	48	31
Dorsomedial prefrontal cortex (dMPFC)	8B	0	34	43
Pre-supplementary motor cortex (pre-SMA)	6	0	18	51
Supplementary motor cortex (SMA)	6	0	1	57

insula demonstrated a different pattern; activation decreased from the anterior insula to the posterior insula, with a stronger gradient being observed in the right hemisphere. Rostro-caudal organization was not observed in the middle and superior frontal gyri (MFG and SFG); in both cases activation was robust in the most caudal ROI (the dorsal premotor cortex, area 6d), and suppressed below baseline or not different from baseline in the remaining ROIs.

2.5. *Goal monitoring*

Fig. 6 illustrates percent signal change values for each ROI when participants received feedback about their progress towards the overarching motivational goal. Clear rostro-caudal organization was present in several brain. Activation in the IFG decreased linearly from rostral to caudal. Activation in the SFG also decreased linearly from rostral (rostrolateral prefrontal cortex, area 10) to caudal (dorsal premotor cortex, area 6d), with a slight bump in activation at the mid-dorsolateral prefrontal cortex (area 9). A strong rostro-caudal gradient was present in the cingulate cortex, with activation decreasing linearly from the pregenual anterior cingulate cortex to the posterior mid-cingulate cortex. In the MPFC, goal monitoring activation was similar across the three most rostral ROIs, and then decreased linearly from the dorsomedial prefrontal cortex (area 8B) to the supplementary motor area. The insula was unique, with goal monitoring activation increasing linearly from rostral to caudal. Finally, a straight-forward pattern was not discernible in the MFG.

2.6. *Time-course analysis*

In our task design, the goal monitoring period always occurred two seconds following the action execution period. As such, a

Table 2 – Results of the ROI statistical analyses.

Brain area	Main effect of ROI	Main effect of hemisphere	ROI × hemisphere	Linear	Quadratic	Cubic
Rule representation						
IFG	$F_{3,42}=12.92$, $p<0.001$	$p>0.19$	$F_{3,42}=3.76$, $p=0.018$	*(R), ***(L)		
MFG	$F_{5,70}=3.90$, $p=0.004$	$p>0.83$	$F_{5,70}=3.84$, $p=0.004$	*(L)		** (L)
SFG	$F_{5,70}=10.08$, $p<0.001$	$F_{1,14}=11.79$, $p=0.004$	$F_{5,70}=2.80$, $p=0.023$	*(L)	*(R), ***(L)	*(R)
Insula	$p=0.19$	$F_{1,14}=5.95$, $p=0.029$	$p>0.95$			
Cingulate	$F_{3,42}=22.64$, $p<0.001$			***		***
MPFC	$F_{4,56}=37.32$, $p<0.001$			***	**	
Rule maintenance						
IFG	$F_{3,42}=3.74$, $p=0.018$	$F_{1,14}=6.92$, $p=0.02$	$p>0.62$	*		
MFG	$p>0.13$	$p>0.31$	$p>0.49$			
SFG	$F_{5,70}=4.88$, $p=0.001$	$p>0.22$	$p>0.76$			*
Insula	$F_{2,28}=51.63$, $p<0.001$	$p>0.72$	$p>0.20$	***		
Cingulate	$F_{3,42}=4.06$, $p=0.013$				***	
MPFC	$F_{4,56}=8.62$, $p<0.001$				**	*
Action execution						
IFG	$F_{3,42}=15.49$, $p<0.001$	$F_{1,14}=24.39$, $p<0.001$	$p>0.80$	***	*	
MFG	$F_{5,70}=28.00$, $p<0.001$	$p>0.35$	$p>0.09$	***	***	***
SFG	$F_{5,70}=38.51$, $p<0.001$	$F_{1,14}=8.47$, $p=0.011$	$F_{5,70}=5.04$, $p=0.001$	***(R)	***(R)	**(L)
				***(L)	***(L)	
Insula	$F_{2,28}=18.57$, $p<0.001$	$F_{1,14}=9.91$, $p=0.007$	$F_{2,28}=4.98$, $p=0.014$	***(R)	** (L)	
Cingulate	$F_{3,42}=40.07$, $p<0.001$			***		*
MPFC	$F_{4,56}=48.10$, $p<0.001$			***		
Goal monitoring						
IFG	$F_{3,42}=17.35$, $p<0.001$	$F_{1,14}=25.84$, $p<0.001$	$p>0.54$	***		
MFG	$F_{5,70}=17.66$, $p<0.001$	$F_{1,14}=8.06$, $p=0.013$	$p>0.81$	***	*	***
SFG	$F_{5,70}=19.66$, $p<0.001$	$F_{1,14}=11.50$, $p=0.004$	$p>0.41$	***		*
Insula	$F_{2,28}=8.77$, $p=0.001$	$p>0.10$	$p=0.088$	**		
Cingulate	$F_{3,42}=16.88$, $p<0.001$			***		
MPFC	$F_{4,56}=41.56$, $p<0.001$			***	***	

Note: All trend analyses (e.g., linear) pertain to the main effect of ROI. When an interaction was present in the ROI × hemisphere ANOVA, we examined the effect of ROI for each hemisphere separately, and report trends accordingly, with (L) denoting a trend in the left hemisphere, and (R) denoting a trend in the right hemisphere.
* $p<0.05$.
** $p<0.005$.
*** $p<0.001$.

potential concern is that the first level GLM analysis (which is the basis for the subsequent ROI analysis) may not have been able to accurately distinguish activation patterns for these events, thus biasing our results. We therefore examined the raw fMRI signal time-course from several ROIs to ensure that this was not the case (see Section 4.10 Time-course analysis). If the pattern we observed is real, then caudal brain areas should show a peak in activation at about 6–10 s following the onset of the action execution period, and rostral areas should show a peak in activation at a *clearly later time-point*, i.e., at 6–10 s following the onset of the goal monitoring period. That is, there should be a systematic shift in peak activation time for rostral relative to caudal areas. We examined a pair of ROIs from the lateral prefrontal cortex and a pair of ROIs from the cingulate cortex and indeed found this to be to be the case.

BOLD signal in caudal ROIs (the dorsal premotor cortex and posterior mid-cingulate cortex) exhibited a peak in activation at 6–8 s following onset of the action execution period, consistent with a strong response during the action execution period, once the hemodynamic lag is accounted for (Fig. 7). In contrast, BOLD signal in the rostral ROIs (the rostrolateral prefrontal cortex and pregenual cingulate cortex) was negligible during this same period, and then exhibited a later rise in activation at 10–14 s, consistent with a response specifically evoked by the goal monitoring period (once the hemodynamic lag is accounted for) (Fig. 7). The timecourse analysis thus provides strong evidence that the pattern of brain activation we observed in the main analysis is not a statistical artifact; rather, the pattern indicates that rostral and caudal brain areas are sensitive to different cognitive processes. Moreover, it is important to note that our main analyses were based on comparing rostral and caudal ROIs during the same trial event, and never based on comparing how a given ROI responded across different trial events.

2.7. *Hemispheric asymmetries*

The purpose of the present investigation was not to probe differences across the left and right hemispheres. However, for completeness, we note that asymmetries emerged in

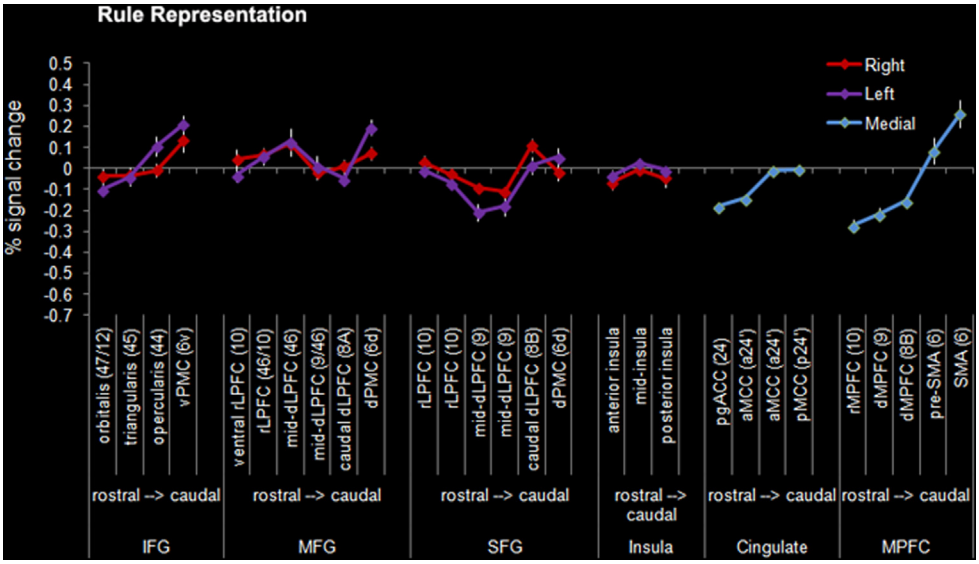

Fig. 3 – ROI activation patterns during rule representation. Percent signal change values are plotted for each ROI. A linear increase in activation from rostral to caudal is evident in the left IFG, MPFC, and to some extent in the cingulate cortex. Error bars reflect one within-participant standard error of the mean based on Loftus and Masson (1994).

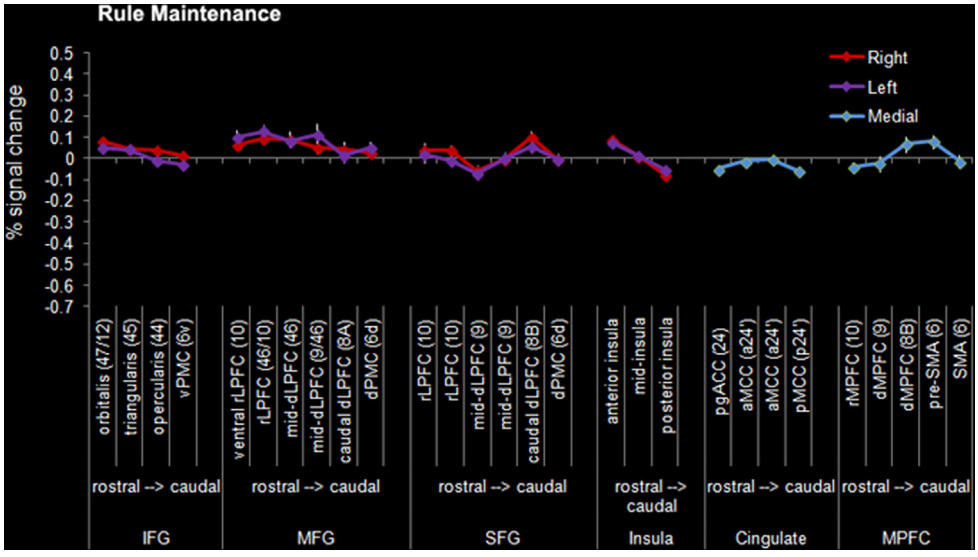

Fig. 4 – ROI activation patterns during rule maintenance. Percent signal change values are plotted for each ROI. There was very little variance across ROIs in activation during rule maintenance. Error bars reflect one within-participant standard error of the mean based on Loftus and Masson (1994).

several brain areas. Most notably, action execution activation was greater in the left compared to the right hemisphere in the IFG, caudal SFG, and mid/posterior insula, whereas goal monitoring activation was greater in the right relative to the left hemisphere in the IFG, MFG, SFG, and mid/posterior insula. Such differences deserve further examination in future work.

3. Discussion

Our findings provide strong evidence that several key brain areas related to goal-directed behavior are organized along a rostro-caudal axis. In every area examined (except the MFG), rostral and caudal ROIs exhibited differential activation patterns when participants executed an action, and also when participants monitored progress towards an overarching motivational goal. In most cases, a significant linear trend was observed, with activation progressively increasing or decreasing from caudal ROIs to rostral ROIs. Importantly, these rostro-caudal gradients were observed during *individual trial events*, and therefore, cannot be explained by task difficulty or other extraneous factors. As such, these findings provide compelling evidence in favor of rostro-caudal organization in multiple regions related to goal-directed behavior.

Is there a way to reconcile studies that have and have not observed rostro-caudal organization? Prior studies have typically used task conditions that varied along a chosen

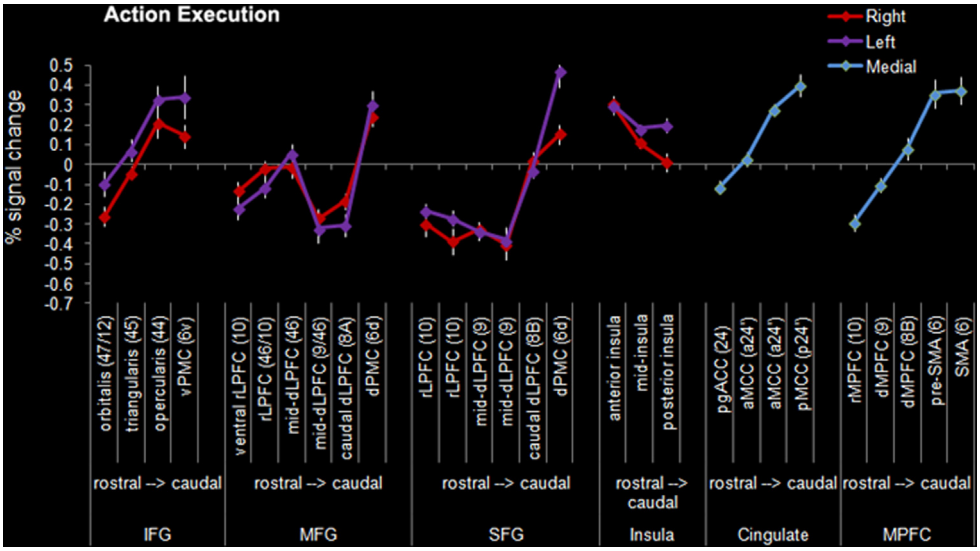

Fig. 5 – ROI activation patterns during action execution. Percent signal change values are plotted for each ROI. Activation increased linearly from rostral to caudal in the IFG, cingulate, and MPFC, and decreased linearly in the insula. Error bars reflect one within-participant standard error of the mean based on Loftus and Masson (1994).

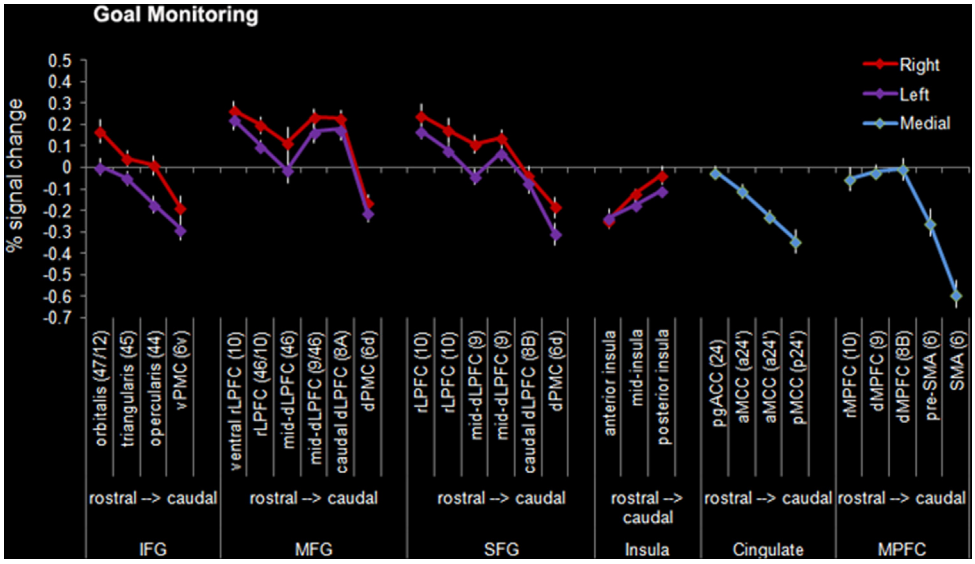

Fig. 6 – ROI activation patterns during goal monitoring. Percent signal change values are plotted for each ROI. Activation decreased linearly from rostral to caudal in the IFG, SFG, cingulate, and MPFC, and increased linearly in the insula. Error bars reflect one within-participant standard error of the mean based on Loftus and Masson (1994).

theoretical dimension to dissociate the functions of rostral and caudal regions. One possibility is that there is an inherent rostro-caudal organization and null findings have resulted from choosing a theoretical orientation that did not capture this inherent organization. One seemingly problematic finding for the rostro-caudal account is that a simple manipulation of task difficulty can result in widespread increases in multiple demand network activation (Crittenden and Duncan, 2014). However, that study did not provide evidence that caudal and rostral regions were influenced by the difficulty manipulation in the same way. It is quite possible that even a simple manipulation of difficulty invokes greater processing at many levels of complexity/abstraction that could be differentially supported by rostral and caudal regions. For example, increased difficulty could lead to greater attention to executed responses to ensure correct performance (putatively causing greater activation in caudal regions), but could also lead to greater attention to the abstract goal of performing well and strategies for optimizing performance (putatively causing greater activation in rostral regions).

An additional possibility to consider is that both the rostro-caudal organization and the multiple demand network accounts are partially correct. We propose that rostro-caudal organization is *emergent*, i.e., it is dependent on task requirements and emerges in some circumstances, but is absent in

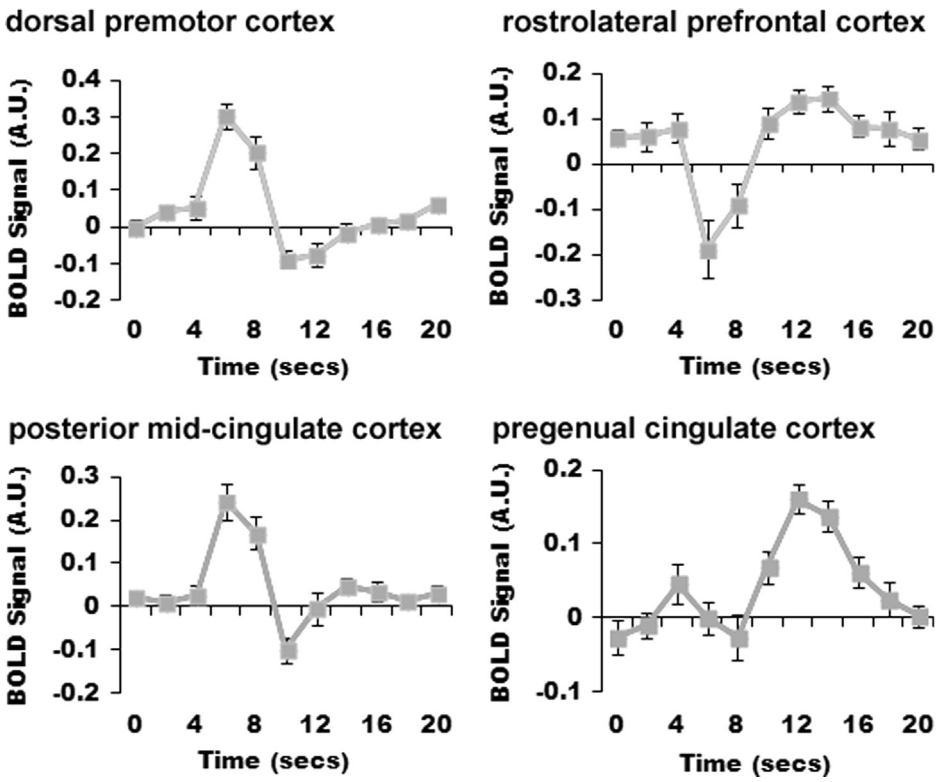

Fig. 7 – Raw BOLD signal time-locked to the action execution period. The raw time-course is plotted for several ROIs. BOLD Signal (in arbitrary units) is time-locked to the onset of the action execution period. Notably, the caudal ROIs (the dorsal premotor cortex and the posterior mid-cingulate cortex) exhibit an early rise in activation that corresponds to the action execution period. In contrast, the rostral ROIs (the rostrolateral prefrontal cortex and the pregenual cingulate cortex) exhibit a later rise in activation that corresponds to the goal monitoring period. The clear difference in the timing of peak activation in the rostral and caudal ROIs supports the idea that they are sensitive to different cognitive operations.

others (see also Christoff and Keramatian, 2007). According to this account, regions along the rostro-caudal axis of a given brain area have the capacity to process similar types of information and perform similar functions, but have slight inherent biases in the type of information that they "prefer" to represent, how efficiently they do so, and the computations they perform. This account predicts that rostro-caudal functional distinctions may be most evident for tasks that can be easily partitioned into different types of information (e.g., concrete versus more abstract information).

3.1. *Rostro-caudal organization when executing actions and monitoring goals*

We found strong differences in activation between caudal and rostral ROIs in several regions when participants executed an action. In the inferior frontal gyrus (IFG), cingulate cortex, and medial prefrontal cortex (MPFC), activation was robust in caudal ROIs (which correspond to lateral, medial, and cingulate premotor areas), and progressively diminished moving to the rostral ROIs. A similar albeit less pronounced pattern was observed in these regions during rule representation. These findings suggest that these caudal regions are involved in translating task rules into specific actions. Moreover, with increasing distance from these premotor areas, activation became progressively less related to action selection. Conversely, when participants were provided with feedback regarding their current progress towards an overarching motivational goal, activation was strongest in rostral ROIs and progressively diminished moving towards caudal ROIs in the IFG, superior frontal gyrus (SFG), cingulate cortex, and MPFC.

Our findings are consistent with prior work demonstrating that the caudal lateral prefrontal cortex (LPFC) is involved in the conditional selection of actions on the basis of their association with visual stimuli, whereas the rostral LPFC represents more complex/abstract rules and goals that govern behavior across longer time-scales (Badre, 2008; Badre and D'Esposito, 2007, 2009; Christoff and Gabrieli, 2000; Christoff and Keramatian, 2007; Christoff et al., 2009; Eiselt and Nieder, 2013; Koechlin et al., 2003; Kouneiher et al., 2009; Petrides, 2005; Race et al., 2009; Yamagata et al., 2012). With regards to the cingulate/MPFC, prior work suggests that the caudal cingulate/MPFC is involved in selecting actions based on their association with desired outcomes, whereas the rostral cingulate/MPFC is involved in representing performance strategies, intentions, and mental states – abstract information that might provide an overarching context for selecting actions (Haynes et al., 2007; Kouneiher et al., 2009; Morecraft and Tanji, 2009; Passingham et al., 2010; Picard and Strick, 1996; Rushworth et al., 2007; Shima and Tanji, 1998; Spunt et al., 2010; Venkatraman et al., 2009). Interestingly, of all the regions we examined, the rostrolateral prefrontal cortex (rLPFC) exhibited the strongest activation when participants were provided with feedback about their cumulative monetary earnings (i.e., their progress

toward the overall motivational goal). Consistent with this, recent studies have observed rLPFC activation during reward processing and decision making, particularly when a future reward is involved (Badre et al., 2012; Boorman et al., 2009; Daw et al., 2006; Diekhof and Gruber, 2010; Jimura et al., 2013; McClure et al., 2004). To summarize, our findings complement prior work examining rostro-caudal organization in the LPFC, cingulate cortex, and MPFC, and provide an important contribution to this literature by supplying evidence of rostro-caudal gradients during individual trial events, and not relying on comparing activation patterns across different task conditions that may be confounded with difficulty.

We also found evidence for rostro-caudal organization this insula, however, the pattern differed from the aforementioned regions. In the left hemisphere, action execution activation was robust along the entire rostro-caudal axis, although it was greatest in the anterior insula. In the right hemisphere, action execution activation was strongest in the anterior insula and decreased linearly across mid and posterior insula. Existing work suggests that viscero-somatic information becomes progressively refined and integrated with cognitive control signals from the posterior to the anterior insula (Cauda et al., 2011, 2012; Chang et al., 2013; Craig, 2002; Critchley et al., 2004; Dosenbach et al., 2006; Farb et al., 2013; Menon and Uddin, 2010; Singer et al., 2004). Our results are consistent with this work, and suggest that the insula may be particularly involved in coordinating viscero-somatic changes (e.g., heart rate, respiratory rate, etc.) specifically during the execution of goal-directed actions. This idea is supported by recent work showing that microstimulation of the monkey insula elicits overt motor programs (e.g., ingestive, disgusted, affiliative, etc.), accompanied by changes in heart rate (Jezzini et al., 2012). One possibility is that the anterior insula translates goal-directed intentions into the appropriate viscero-somatic patterns, and then the mid/posterior insula initiates these changes via descending projections to the ventromedial thalamus and other interoceptive regions.

3.2. *Functional organization of the LPFC*

While our findings generally support the idea of rostro-caudal organization in the LPFC, they also suggest independent streams of functional organization along its constituent gyri. In particular, evidence of rostro-caudal organization was observed for the inferior and superior frontal gyri, but not for the middle frontal gyrus. Of course it remains possible that the middle frontal gyrus may exhibit rostro-caudal organization under different task demands than those assessed here. Nevertheless, our findings suggest that it is important to decompose the LPFC into its constituent gyri and consider each as a separate stream of functional organization. This finding is broadly consistent with a recent study showing that the ventral and dorsal LPFC exhibited independent rostro-caudal patterns of intrinsic functional connectivity with the dorsal cingulate/MPFC (Blumenfeld et al., 2012).

3.3. *Anatomical basis of rostro-caudal organization*

A key issue remaining for future work is to discern the underlying anatomical and physiological properties that give rise to rostro-caudal organization. Some existing findings provide some hints as to the anatomical basis of rostro-caudal organization. If rostral subregions support more complex/abstract representations that hierarchically govern processing in caudal subregions, then two predictions can be made: (1) rostral subregions should receive more highly processed multimodal afferent input and (2) rostral subregions should have more widespread efferent projections that allow them to differentially influence caudal subregions (Badre and D'Esposito, 2009). With respect to the first prediction, there is some evidence that the rostro-caudal organization of the frontal cortex is reflected in terms of patterns of connectivity with other regions of the brain. For example, progressively more rostral subregions of the LPFC are preferentially connected with progressively more rostral parts of the temporal cortex (Christoff and Keramatian, 2007). This topographic organization of connectivity is consistent with the idea that rostral subregions of the LPFC receive more highly processed multimodal sensory input than caudal subregions (Christoff and Keramatian, 2007).

With respect to the second prediction, rostral subregions (areas 10, 9, and 46) of the LPFC exhibit less laminar differentiation (i.e., the extent to which cells are organized into cortical layers) than caudal subregions (areas 9/46 and 8), and there is some evidence that less differentiated areas tend to have more widespread anatomical connections, whereas more differentiated areas tend to have more limited connections that preferentially target neighboring regions (Badre and D'Esposito, 2009). Indeed the efferent projections of rostral area 10 go beyond its immediate neighbors to reach caudal area 6, whereas the converse is not the case; area 6 does not directly project to area 10. This pattern is consistent with rostral area 10 exerting a hierarchical influence on caudal area 6 (Badre and D'Esposito, 2009). Although more work is required, these anatomical findings provide some preliminary information regarding the underlying basis of rostro-caudal organization.

3.4. *Limitations*

Several methodological limitations are worth noting. First, the ROIs were based on a template brain rather than individual participant's unique anatomy. Therefore, references to specific architectonic regions should be taken as an *approximation* of anatomical locations only. Importantly, this does not affect our central conclusions about the presence and form of the rostro-caudal gradients. Second, the feedback period presented information about money earned on that trial and also cumulative winnings. We favor the interpretation that participants were focusing mainly on their cumulative winnings (i.e., progress towards the overarching motivational goal) given that we emphasized to participants that this was the relevant information to which they should devote their attention. However, activation during this time period could also potentially reflect trial-specific feedback in addition to monitoring the overarching motivational goal. Notably, the precise interpretation is of secondary importance; the key point is that we found evidence that rostral and caudal ROIs exhibited differential activation during this trial event. An additional issue is that we strictly examined rostro-caudal gradients; it is very likely that other gradients (e.g., dorsal-ventral; arcuate) also exist (e.g., Christoff and Keramatian, 2007; Nicolle et al., 2012; Petrides, 2005), and these deserve further examination. Finally, it will be important

for future work to examine additional brain areas and to utilize additional task events to provide a more complete picture of functional organization across the numerous brain areas that contribute to goal-directed behavior.

3.5. Conclusion

Our results provide compelling evidence that multiple regions related to goal-directed behavior are functionally organized along a rostro-caudal axis. Interestingly, such organization was strongly evident during action execution and goal monitoring. Thus, although each brain area clearly has a unique role to play in goal-directed behavior, the present findings are suggestive of a common organizing principle for rostro-caudal gradients. A simple heuristic is that caudal regions – in close proximity to primary sensory-motor and interoceptive cortices – support concrete sensory-motor-homeostatic programs that are executed during interactions with the environment, whereas rostral regions support more abstract evaluative processes that guide the adaptive selection of these programs based on desired outcomes. This idea is consistent with the suggestion that rostro-caudal gradients in the prefrontal cortex reflect a hierarchical organization (Badre and D'Esposito, 2009; Christoff and Gabrieli, 2000). Interestingly, the fact that linear trends were frequently observed suggests a gradual, rather than qualitative, transition from concrete action-related representations to more abstract goal representations. Thus, abstract goal representations may be an extension or elaboration of concrete sensory-motor-homeostatic mechanisms that adaptively regulate a body interacting with the world (Barsalou, 2008; Pezzulo et al., 2012; Thompson, 2005).

4. Experimental procedures

4.1. Participants

Participants were 15 (right-handed) healthy adults ($M=27.4$ years, $SD=5.51$ years; 8 female), with no history of psychiatric or neurological illness. All participants understood the requirements of the experiment and provided written informed consent and received payment for their participation. The study was approved by the UBC clinical research ethics board.

4.2. Task design

On each trial, participants indicated whether a face was male/female or indicated whether a word had an abstract/concrete meaning (see Fig. 1). Thus, simple 'if–then' type rules were required (e.g., if face task and if male then press button "1", if female press button "2"). On some trials, money (25 cents) was available to be earned, contingent on performance (accurate response within a 1400 ms time-window). Participants could earn up to $60 in total by the end of the task ($30 guaranteed payment+up to $30 based on task performance). Trials started with a jittered interstimulus interval (mean=4.9 s, range=2–7.5 s, increments of 500 ms). This was followed by an instruction cue (2 s) indicating the relevant rules and whether or not to expect a monetary reward (we refer to this time period as "rule representation"). This was followed by a 4–6 s (mean=5 s) delay period ("rule maintenance"). Participants then made a button response during presentation (2 s) of the word or face stimulus ("action execution"). Finally, a feedback screen was presented (1.5 s) indicating total cumulative winnings and also whether money had been earned on that trial. It was emphasized to participants that they should pay particular attention to their progress towards the overarching motivational goal of earning the maximum amount of money available ("goal monitoring"). Notably, the fact that money was earned on some trials but not others supports the idea that brain activation during this period should reflect the process that is common across both of these trial types, namely, monitoring progress towards the overall motivational goal, and should not reflect processing of the specific reward per se. On some trials, a second instruction cue (2 s) appeared followed by a delay (4 s) prior to stimulus presentation. This allowed us to look for fMRI-adaptation which was the focus of a separate report (Dixon and Christoff, 2012). In this report, all instruction cue periods were analyzed together to provide an overall estimate of brain activation during rule processing. Participants performed 162 trials in total, presented pseudorandomly such that no condition (i.e., task rules+expected outcome) appeared more than twice in a row. On 75% of the trials, the participants used the abstract/concrete rule to respond to the stimuli, and on 25% of trials the participants used the male/female rule to respond to the stimuli. The greater number of trials involving the abstract/concrete rule was necessary for examining fMRI-adaptation, which was the focus of a previous report (Dixon and Christoff, 2012). The abstract/concrete rule was signaled by an image of one of two different cartoon books, the male/female rule was signaled by one of two different schematic images of people, the 25 cent monetary reward was signaled by an image of dollar bills or a money bag, and the no monetary reward outcome was signaled by one of two different vases. The purpose of using two different images to signal each rule and outcome was to ensure that evoked brain activation was specifically attributable to rule and outcome processing, and not due to visual processing of the cues. One day prior to scanning, participants received 80 practice trials in order to become familiar with the meaning of the instruction cues. Buttons 1 and 2 were the only buttons used, and the mappings (1=male/abstract, 2=female/concrete) remained constant across subjects.

4.3. Stimuli

Words were chosen from the Medical Research Council Psycholinguistic Database (http://www.psy.uwa.edu.au/mrcdatabase/uwa_mrc.htm). The words had a minimum of three letters and a maximum of eight letters, and a minimum written frequency of 30. Words selected for the "concrete" category (e.g., bag), had a concrete rating above 600 and words selected for the "abstract" category (e.g., advice) had a concrete rating below 300. The face stimuli were high resolution front-view photographs of neutral expression faces obtained from several image databases (Lundqvist et al., 1998; Martinez and Benavente, 1998; Phillips et al., 1998). In total, 42 photographs (21 male, 21 female) were selected. The faces were cropped to remove hair and other non-facial features, gray-scaled, and equated in size. We then added 10% Gaussian noise to increase the difficulty of the face discrimination (making it more comparable to the abstract/

concrete word discrimination task). Stimuli subtended 4.5 (width) × 4.7 (height) degrees visual angle.

4.4. *fMRI data acquisition*

fMRI data were collected using a 3.0-Tesla Philips Intera MRI scanner (Best, Netherlands) with a standard 8-element 6-channel phased array head coil with parallel imaging capability (SENSE). Head movement was restricted using foam padding around the head. T2*-weighted functional images were acquired parallel to the anterior commissure/posterior commissure (AC/PC) line using a single shot gradient echo-planar sequence (repetition time, TR=2 s; echo time, TE=30 ms; flip angle, FA=90°; field of view, FOV=24 × 24 × 14.3 cm^3; matrix size=80 × 80; SENSE factor=1.0). Thirty-six interleaved axial slices covering the whole brain were acquired (3-mm thick with 1-mm skip). Data collected during the first 4 TRs were discarded to allow for equilibration effects. There were six sessions, each approximately nine-minutes long, during which 1608 volumes were acquired in total. After functional imaging, in-plane inversion recovery prepared T1-weighted anatomical images were acquired in the same slice locations as the functional images using a fast spin-echo sequence (TR=2 s; TE=10 ms; 36 interleaved axial slices covering the whole brain, 3-mm thick with 1-mm skip; FA=90°; FOV=22.4 × 22.4 × 14.3 cm^3; matrix size=240 × 235; reconstructed matrix size=480 × 470; inversion delay=800 ms; spin echo turbo factor=5).

4.5. *fMRI data preprocessing*

Image preprocessing and analysis were conducted with Statistical Parametric Mapping (SPM5, University College London, London, UK; http://www.fil.ion.ucl.ac.uk/spm/software/spm5). Time series data were slice-time corrected (to the middle slice), realigned to the first volume to correct for between-scan motion (using a 6 parameter rigid body transformation), and coregistered with the T1-weighted structural image. The in-plane T1 image was bias-corrected and segmented using template (ICBM) tissue probability maps for gray/white matter and CSF. Parameters obtained from this step were subsequently applied to the functional (re-sampled to 3 mm^3 voxels) and structural (re-sampled to 1 mm^3 voxels) data during normalization to MNI space. The data were spatially-smoothed using an 8-mm^3 full-width at half-maximum Gaussian kernel to reduce the impact of inter- participant variability in brain anatomy. Finally, a linear detrending procedure (Macey et al., 2004) was applied to remove time-series components that were correlated with global changes in the BOLD signal.

4.6. *fMRI data analysis: first-level model*

Data were first analyzed at the individual participant level with a general linear model. Four key regressors were convolved with a canonical hemodynamic response function: (1) instruction cues specifying rule representation (modeled by stick functions); (2) delay periods during which rules were maintained in working memory (modeled by variable-duration epochs); (3) action execution (modeled by stick functions); and (4) feedback processing/goal monitoring (modeled by stick functions). It should be noted that on some trials, two instruction cues appeared which allowed us to look at fMRI-adaptation, as described in a previous report (Dixon and Christoff, 2012). However, in the present analysis, the regressor coding the onset of the rules treated all rules the same (i.e., it did not distinguish between the specific nature of the rules) because we were interested in capturing brain activation related to general rule processing. An additional regressor modeled as a variable-duration (10 or 15 s) epoch coded a rest period at the middle and end of each session. The model also included nuisance regressors to remove non-neural influences on the BOLD response, including the six movement parameters estimated during realignment, and timecourse activation from ROIs centered in the ventricles and white matter. Finally, there were regressors coding session effects. The variable duration ISI between each trial was not modeled and served as an implicit baseline. Serial autocorrelations were modeled using AR(1), and the data were high-pass filtered (1/128 Hz) to remove low frequency drift in the BOLD signal.

4.7. *Regions of interest (ROI) selection*

The ROI names and MNI coordinates are listed in Table 1. The inferior frontal gyrus (IFG) ROIs captured the major architectonic regions of the IFG (pars orbitalis, pars triangularis, and pars opercularis), and were identified using macroscopic anatomical landmarks including the horizontal ramus, the ascending ramus, and the inferior precentral sulcus. The ventral premotor cortex (located on the precentral gyrus) was also selected as an ROI given its role in goal-directed motor control. The architectonic territories of the middle and superior frontal gyri (MFG and SFG) are difficult to discern using macroscopic landmarks. Thus, we created approximately equidistant ROIs that spanned the rostrolateral prefrontal cortex to the dorsal premotor cortex, and estimated the corresponding architectonic area using the map of Petrides and Pandya (1999). The insula contains a number of distinct subregions, but can be broadly divided into posterior (granular), mid (dysgranular) and anterior (agranular) regions. The ROIs captured these three divisions. ROIs were defined bilaterally for the IFG, MFG, SFG, and insula. A single set of midline cingulate ROIs was defined, extending from pregenual anterior cingulate cortex to posterior mid-cingulate cortex. The pregenual cingulate sits rostral to the genu of the corpus callosum whereas the mid-cingulate lies above the corpus callosum, with the VCA line (i.e., the vertical plane passing through the anterior commissure) providing the approximate border between the anterior mid-cingulate and the posterior mid-cingulate. Nomenclature for the cingulate ROIs is based on the four-region model of Vogt (2009) and Vogt et al. (2005), which is predicated on architectonic, connectional, and functional considerations. Architectonic regions of MPFC are difficult to identify using macroscopic landmarks; thus, we created approximately equidistant ROIs and estimated the corresponding architectonic area using the map of Petrides and Pandya (1999). It is important to note that all of the ROIs were based on a template brain and not participants' unique anatomy. Therefore, the ROIs represented an approximation of the aforementioned architectonic regions. The coordinates for each ROI were determined based on visual inspection to meet three criteria: (1) we aimed to place the ROI in the center of a given architectonic region; (2) we

aimed to capture only gray matter and not white matter in the ROI; and (3) we aimed to make the ROIs approximately equidistant (~18–20 mm between ROI center coordinates).

4.8. ROI data extraction

The Marsbar toolbox in SPM8 (Brett et al., 2002) (http://marsbar.sourceforge.net/) was used to extract average signal change values from 6-mm radius spheres centered on the ROI coordinates listed in Table 1. Data from all voxels within the ROI were averaged to derive percent signal change values. This was done separately for each trial event that was modeled in the 1st-level GLM analysis. Marsbar calculates signal change by contrasting signal in the ROI during the event of interest with the mean signal in the ROI during the entire time-course. The rule representation, action execution, and goal monitoring periods were modeled as 0 second events, while the rule maintenance period was modeled as a 4 second event. Although the rule maintenance period varied between 4 and 6 s, Marsbar requires events to be modeled with a constant duration, so we selected 4 s; the shortest event length was selected to avoid inclusion of signal during the following action execution period on some trials, which would have occurred had a longer duration been selected.

4.9. ROI-based statistical analyses

For each ROI, we calculated percent signal change values during each of the four task events. For each trial event, we conducted separate repeated measures ANOVAs for each brain area, with ROI and hemisphere (when applicable) as independent variables, and percent signal change as the dependant variable. Rostro-caudal organization was informed through identifying trends that characterized activation patterns across the ROIs, including: linear (a straight line), quadratic (a line with a single bend), and cubic (a line with two bends).

4.10. Time-course analysis

To corroborate the main analyses, we examined the raw fMRI signal time-course in a set of ROIs from the superior frontal gyrus and a set of ROIs from the cingulate cortex: (1) the dorsal premotor cortex (x, y, z = −22, −8, 70) which exhibited stronger activation during action execution relative to goal monitoring in the main analysis; (2) the rostrolateral prefrontal cortex (x, y, z = 22, 66, 13) which exhibited stronger activation during goal monitoring relative to action execution in the main analysis; (3) the posterior mid-cingulate cortex (x, y, z = 0, −1, 40) which exhibited stronger activation during action execution relative to goal monitoring in the main analysis; and (4) the pregenual anterior cingulate cortex (x, y, z = 0, 40, 5) which exhibited stronger activation during goal monitoring relative to action execution in the main analysis. For each ROI, we extracted the raw BOLD signal from 0–20 s following the onset of the action execution period for each trial. The signal was averaged across trials, and then averaged across participants to generate Fig. 7. The rationale was that the caudal ROIs (the dorsal premotor cortex and the posterior mid-cingulate cortex) should exhibit a peak in activation at about 6–10 s, which would correspond to a response elicited by the action execution period once accounting for the hemodynamic lag, whereas the rostral ROIs (the rostrolateral prefrontal cortex and pregenual anterior cingulate cortex) should exhibit a peak activation in activation at about 8–12 s which would correspond to a response elicited by the goal monitoring period once accounting for the hemodynamic lag.

Acknowledgments

This work was supported by the Natural Sciences and Engineering Council of Canada (NSERC; Grant # 05-5918) and the Institute of Neurosciences, Mental Health and Addiction (INMHA; Bridge Grant # 112361) to K.C. The authors declare that there were no conflicts of interest.

REFERENCES

Badre, D., 2008. Cognitive control, hierarchy, and the rostro-caudal organization of the frontal lobes. Trends Cogn. Sci. 12 (5), 193–200.

Badre, D., D'Esposito, M., 2007. Functional magnetic resonance imaging evidence for a hierarchical organization of the prefrontal cortex. J. Cogn. Neurosci. 19 (12), 2082–2099.

Badre, D., D'Esposito, M., 2009. Is the rostro-caudal axis of the frontal lobe hierarchical?. Nat. Rev. Neurosci. 10 (9), 659–669.

Badre, D., Doll, B.B., Long, N.M., Frank, M.J., 2012. Rostrolateral prefrontal cortex and individual differences in uncertainty-driven exploration. Neuron 73 (3), 595–607.

Barsalou, L.W., 2008. Grounded cognition. Annu. Rev. Psychol. 59, 617–645.

Blumenfeld, R.S., Nomura, E.M., Gratton, C., D'Esposito, M., 2012. Lateral prefrontal cortex is organized into parallel dorsal and ventral streams along the rostro-caudal axis. Cereb. Cortex.

Boorman, E.D., Behrens, T.E., Woolrich, M.W., Rushworth, M.F., 2009. How green is the grass on the other side? Frontopolar cortex and the evidence in favor of alternative courses of action. Neuron 62 (5), 733–743.

Brett, M., Anton, J.-L., Valabregue, R., & Poline, J.-B., June 2–6, 2002. Region of interest analysis using an SPM toolbox [abstract]. Paper Presented at the 8th International Conference on Functional Mapping of the Human Brain.

Bunge, S.A., Kahn, I., Wallis, J.D., Miller, E.K., Wagner, A.D., 2003. Neural circuits subserving the retrieval and maintenance of abstract rules. J. Neurophysiol. 90 (5), 3419–3428.

Cauda, F., Costa, T., Torta, D.M., Sacco, K., D'Agata, F., Duca, S., et al., 2012. Meta-analytic clustering of the insular cortex: characterizing the meta-analytic connectivity of the insula when involved in active tasks. Neuroimage 62 (1), 343–355.

Cauda, F., D'Agata, F., Sacco, K., Duca, S., Geminiani, G., Vercelli, A., 2011. Functional connectivity of the insula in the resting brain. Neuroimage 55 (1), 8–23.

Chang, L.J., Yarkoni, T., Khaw, M.W., Sanfey, A.G., 2013. Decoding the role of the insula in human cognition: functional parcellation and large-scale reverse inference. Cereb. Cortex 23 (3), 739–749.

Christoff, K., Gabrieli, J.D.E., 2000. The frontopolar cortex and human cognition: evidence for a rostrocaudal hierarchical organization within the human prefrontal cortex. Psychobiology 28 (2), 168–186.

Christoff, K., Keramatian, K., 2007. Abstraction of mental representations: theoretical considerations and neuroscientific evidence. In: Bunge, S.A., Wallis, J.D. (Eds.), Rule-Guided Behavior. Oxford University Press.

Christoff, K., Keramatian, K., Gordon, A.M., Smith, R., Madler, B., 2009. Prefrontal organization of cognitive control according to levels of abstraction. Brain Res. 1286, 94–105.
Cole, M.W., Schneider, W., 2007. The cognitive control network: integrated cortical regions with dissociable functions. Neuroimage 37 (1), 343–360.
Craig, A.D., 2002. How do you feel? Interoception: the sense of the physiological condition of the body. Nat. Rev. Neurosci. 3 (8), 655–666.
Critchley, H.D., Wiens, S., Rotshtein, P., Ohman, A., Dolan, R.J., 2004. Neural systems supporting interoceptive awareness. Nat. Neurosci. 7 (2), 189–195.
Crittenden, B.M., Duncan, J., 2014. Task difficulty manipulation reveals multiple demand activity but no frontal lobe hierarchy. Cereb. Cortex 24 (2), 532–540.
Daw, N.D., O'Doherty, J.P., Dayan, P., Seymour, B., Dolan, R.J., 2006. Cortical substrates for exploratory decisions in humans. Nature 441 (7095), 876–879.
Diekhof, E.K., Gruber, O., 2010. When desire collides with reason: functional interactions between anteroventral prefrontal cortex and nucleus accumbens underlie the human ability to resist impulsive desires. J. Neurosci. 30 (4), 1488–1493.
Dixon, M.L., Christoff, K., 2012. The decision to engage cognitive control is driven by expected reward-value: neural and behavioral evidence. PLOS One 7 (12), 1–12.
Dixon, M.L., Christoff, K., 2014. The lateral prefrontal cortex and complex value-based learning and decision making. Neurosci Biobehav Rev. 45, 9–18, http://dx.doi.org/10.1016/j.neubiorev.2014.04.011.
Dosenbach, N.U., Visscher, K.M., Palmer, E.D., Miezin, F.M., Wenger, K.K., Kang, H.C., et al., 2006. A core system for the implementation of task sets. Neuron 50 (5), 799–812.
Duncan, J., 2010. The multiple-demand (MD) system of the primate brain: mental programs for intelligent behaviour. Trends Cogn. Sci. 14 (4), 172–179.
Eiselt, A.K., Nieder, A., 2013. Rule activity related to spatial and numerical magnitudes: comparison of prefrontal, premotor, and cingulate motor cortices. J. Cogn. Neurosci. 26 (5), 1000–1012.
Farb, N.A., Segal, Z.V., Anderson, A.K., 2013. Attentional modulation of primary interoceptive and exteroceptive cortices. Cereb. Cortex 23 (1), 114–126.
Farooqui, A.A., Mitchell, D., Thompson, R., Duncan, J., 2012. Hierarchical organization of cognition reflected in distributed frontoparietal activity. J. Neurosci. 32 (48), 17373–17381.
Haynes, J.D., Sakai, K., Rees, G., Gilbert, S., Frith, C., Passingham, R.E., 2007. Reading hidden intentions in the human brain. Curr. Biol. 17 (4), 323–328.
Jezzini, A., Caruana, F., Stoianov, I., Gallese, V., Rizzolatti, G., 2012. Functional organization of the insula and inner perisylvian regions. Proc. Natl. Acad. Sci. USA 109 (25), 10077–10082.
Jimura, K., Chushak, M.S., Braver, T.S., 2013. Impulsivity and self-control during intertemporal decision making linked to the neural dynamics of reward value representation. J. Neurosci. 33 (1), 344–357.
Koechlin, E., Ody, C., Kouneiher, F., 2003. The architecture of cognitive control in the human prefrontal cortex. Science 302 (5648), 1181–1185.
Kouneiher, F., Charron, S., Koechlin, E., 2009. Motivation and cognitive control in the human prefrontal cortex. Nat. Neurosci. 12 (7), 939–945.
Loftus, G.R., Masson, E.J.M., 1994. Using confidence intervals in within–subject designs. Psychon. Bull. Rev. 1, 476–490.
Lundqvist, D., Flykt, A., Ohman, A., 1998. Karolinska Directed Emotional Faces [Database of standardized facial images]. Psychology Section. Department of Clinical Neuroscience, Karolinska Hospital, Stockholm, Sweden.
Macey, P.M., Macey, K.E., Kumar, R., Harper, R.M., 2004. A method for removal of global effects from fMRI time series. Neuroimage 22 (1), 360–366.
Martinez, A.M., Benavente, R.,1998. The AR Face Database. CVC Technical Report #24.
McClure, S.M., Laibson, D.I., Loewenstein, G., Cohen, J.D., 2004. Separate neural systems value immediate and delayed monetary rewards. Science 306 (5695), 503–507.
Menon, V., Uddin, L.Q., 2010. Saliency, switching, attention and control: a network model of insula function. Brain Struct. Funct. 214 (5-6), 655–667.
Morecraft, R.J., Tanji, J., 2009. Cingulofrontal interactions and the cingulate motor areas. In: Vogt, B.A. (Ed.), Cingulate Neurobiology and Disease. Oxford University Press, Oxford, New York, pp. 113–144.
Nicolle, A., Klein-Flugge, M.C., Hunt, L.T., Vlaev, I., Dolan, R.J., Behrens, T.E., 2012. An agent independent axis for executed and modeled choice in medial prefrontal cortex. Neuron 75 (6), 1114–1121.
Passingham, R.E., Bengtsson, S.L., Lau, H.C., 2010. Medial frontal cortex: from self-generated action to reflection on one's own performance. Trends Cogn. Sci. 14 (1), 16–21.
Petrides, M., 2005. Lateral prefrontal cortex: architectonic and functional organization. Philos. Trans. R. Soc. Lond. B Biol. Sci. 360 (1456), 781–795.
Petrides, M., Pandya, D.N., 1999. Dorsolateral prefrontal cortex: comparative cytoarchitectonic analysis in the human and the macaque brain and corticocortical connection patterns. Eur. J. Neurosci. 11 (3), 1011–1036.
Pezzulo, G., Barsalou, L.W., Cangelosi, A., Fischer, M.H., McRae, K., Spivey, M.J., 2012. Computational grounded cognition: a new alliance between grounded cognition and computational modeling. Front. Psychol. 3, 612.
Phillips, P.J., Wechsler, H., Huang, J., Rauss, P.J., 1998. The FERET database and evaluation procedure for face-recognition algorithms. Image Vis. Comput. 16 (5), 295–306.
Picard, N., Strick, P.L., 1996. Motor areas of the medial wall: a review of their location and functional activation. Cereb. Cortex 6 (3), 342–353.
Race, E.A., Shanker, S., Wagner, A.D., 2009. Neural priming in human frontal cortex: multiple forms of learning reduce demands on the prefrontal executive system. J. Cogn. Neurosci. 21 (9), 1766–1781.
Reynolds, J.R., O'Reilly, R.C., Cohen, J.D., Braver, T.S., 2012. The function and organization of lateral prefrontal cortex: a test of competing hypotheses. PLOS One 7 (2), e30284.
Rushworth, M.F., Behrens, T.E., Rudebeck, P.H., Walton, M.E., 2007. Contrasting roles for cingulate and orbitofrontal cortex in decisions and social behaviour. Trends Cogn. Sci. 11 (4), 168–176.
Shima, K., Tanji, J., 1998. Role for cingulate motor area cells in voluntary movement selection based on reward. Science 282 (5392), 1335–1338.
Singer, T., Seymour, B., O'Doherty, J., Kaube, H., Dolan, R.J., Frith, C.D., 2004. Empathy for pain involves the affective but not sensory components of pain. Science 303 (5661), 1157–1162.
Spunt, R.P., Falk, E.B., Lieberman, M.D., 2010. Dissociable neural systems support retrieval of how and why action knowledge. Psychol. Sci. 21 (11), 1593–1598.
Thompson, E., 2005. Sensorimotor subjectivity and the enactive approach to experience. Phenomenol. Cogn. Sci. 4, 407–427.
Venkatraman, V., Rosati, A.G., Taren, A.A., Huettel, S.A., 2009. Resolving response, decision, and strategic control: evidence for a functional topography in dorsomedial prefrontal cortex. J. Neurosci. 29 (42), 13158–13164.
Vogt, B.A., 2009. Regions and subregions of the cingulate cortex. In: Vogt, B.A. (Ed.), Cingulate Neurobiology

and Disease. Oxford University Press, Oxford; New York, pp. 3–30.
Vogt, B.A., Vogt, L., Farber, N.B., Bush, G., 2005. Architecture and neurocytology of monkey cingulate gyrus. J. Comp. Neurol. 485 (3), 218–239.
Yamagata, T., Nakayama, Y., Tanji, J., Hoshi, E., 2012. Distinct information representation and processing for goal-directed behavior in the dorsolateral and ventrolateral prefrontal cortex and the dorsal premotor cortex. J. Neurosci. 32 (37), 12934–12949.